

Collective Motion in the Interfacial and Interior Regions of Supported Polymer Films and its Relation to Relaxation

Wengang Zhang,^{*,†} Francis W. Starr,^{*,‡} and Jack F. Douglas^{*,†}

[†]*Materials Science and Engineering Division, National Institute of Standards and Technology, Gaithersburg, Maryland 20899*

[‡]*Department of Physics, Wesleyan University, Middletown, Connecticut 06459-0155*

E-mail: wzhang01@wesleyan.edu; fstarr@wesleyan.edu; jack.douglas@nist.gov

Abstract

To understand the role of collective motion in the often large changes in interfacial molecular mobility observed in polymer films, we investigate the extent of collective motion in the interfacial regions of a thin supported polymer film and within the film interior by molecular dynamics simulation. Contrary to commonly stated expectations, we find that the extent of collective motion, as quantified by string-like molecular exchange motion, is similar in magnitude in the polymer-air interfacial layer as the film interior, and distinct from the bulk material. This finding is consistent with Adam-Gibbs description of the segmental dynamics within mesoscopic film regions where the extent of collective motion is related to the configurational entropy of the film as *whole* rather than a locally defined extent of collective motion or configurational entropy.

It is generally appreciated that thin supported polymer films, and other polymeric nanoconfined materials (nanocomposites, spherical polymer nanoparticles, polymer nanotubes, etc.),

exhibit large gradients of mobility in their interfacial regions that can greatly influence their end-use properties.¹⁻⁵ Typically, depending on the type of interface and the nature and magnitude of the interaction strength and the material properties of the surrounding medium, the scale of the interfacial regions⁶ with altered mobility is on the order of a few nm, and the relaxation time in the interfacial region of glass-forming materials can differ from the overall relaxation time of the film by a factor⁷⁻¹¹ as large as 10^7 . Since mobility gradients in thin films can evidently be quite large, it is not surprising that this phenomenon has elicited significant research interest from both theoretical and practical perspectives.

Changes in mobility of this magnitude can be rationalized within a widely utilized framework for understanding the slowing down of relaxation in bulk glass-forming liquids introduced by Adam and Gibbs (AG).¹² Specifically, a dramatic enhancement of mobility might be interpreted in terms of a reduction of the scale of collective motion in thin films, and some evidence for a reduced degree of collective motion has been reported based on molecular dynamics simulations.^{13,14} However, this former work did not consider how collective motion is altered in the interfacial region, but only for the film as a whole. In particular, Riggleman et al.¹⁵ observed the scale of collective motion in thin polymer films to decrease somewhat as the films were made thinner, a trend notably contrary to what one might naively expect from the Gibbs-DiMarzio model of glass-formation¹⁶ where a reduction of system dimensionality should lead to a reduction of the configurational entropy S_c of fluid,¹⁷ and a corresponding increase of the glass transition temperature. The fact that many experimental studies indicate an apparent depression of the glass transition temperature T_g is often taken as a point against the configurational entropy description of glass-formation.¹⁸ However, this criticism does not apply to the Adam-Gibbs model where structural relaxation time depends both on the activation free energy in the high temperature fluids ($\Delta\mu$) and S_c . We shall see below that $\Delta\mu$ plays a central role in understanding the dynamics of our thin films.

The identification of large structural relaxation times with a relatively high degree of collective motion has often been taken to imply that collective motion in the polymer-air

interfacial region should be greatly suppressed with respect to the interior of the film,^{19–22} and Forest and coworkers^{19,23} have recently introduced a model of the interfacial dynamics of glassy materials based on a combination of the Adam-Gibbs model and the free volume model²⁴ of glass-formation, in which a direct relation between local density and mobility is postulated. A number of authors have reported relaxation in the polymer-air interfacial region to be more nearly Arrhenius than the relaxation of the film as a whole,^{10,25,26} seemingly supporting this interpretation of high interfacial mobility. However, this attractive interpretation of the mobility gradient in the interfacial regions of polymer materials raises a fundamental question with regard to the AG model of glass-formation, since the scale of collective motion (defined by the number of molecules involved in cooperative rearrangement) is predicted to scale inversely with the configurational entropy, arguably a property of the film as a whole (as opposed to being defined locally). We may then expect that the scale of collective motion to be the *same* in the film interfacial regions and the film interior.

Based on these considerations, it is a matter of theoretical and practical interest to quantify how cooperative motion, identified in many earlier works as string-like particle exchange motion,^{27–33} varies in the interfacial and interior regions of model thin supported polymer films. We consider a range of film thicknesses and polymer substrate interaction strengths to evaluate the extent to which AG ideas apply in highly confined materials. We find that, while the average string length L is reduced relative to the bulk material, L varies only weakly when averaged over the interfacial region compared to that of the film interior.

Thus, the large mobility gradients in the film profile are not accompanied by a corresponding variation in cooperative motion. Evidently, the large mobility gradient in the interfacial regions arises from the spatial variation of the *activation enthalpy and entropy within the film*, an effect that persists even at elevated temperature,⁵ and which depends on the boundary interaction strength and film thickness. These activation free energy parameters then exert a significant influence on changes of the dynamics observed in thin films, as observed in an earlier study.³⁴

Since the idea of a gradient in the extent of collective motion near interfaces is an intuitively attractive concept, we also explore the degree of collective motion layer by layer by binning the strings according to their center of mass positions normal to the interface to define a “local” measure of the extent of collective motion in the inset of Fig. 4. Unfortunately, this measure of local collective motion does not seem to inform about layer by layer variations of segmental mobility (see inset of Fig. 1). This finding is reminiscent of our previous observation³⁵ that the local density, as defined by local Voronoi volume neighborhoods, is also not predictive of local molecular mobility. Moreover, previous work has also shown that the gradient of the local density in the interfacial region of films does not correlate strongly with the interfacial mobility gradient.^{34,36}

Results and Discussion

Our findings are based on an analysis of molecular dynamics simulations of thin polymer films with variable polymer-substrate interaction strength ε and film thickness h . These simulations have been described in earlier work.^{38,39} In brief, we study simulated supported films composed of a collection of coarse-grained polymers. These polymer films consist of 320, 400, 480, or 600 polymer chains with film thicknesses $h \approx 8\sigma$, 10σ , 12σ , and 15σ , respectively. We refer to these film as $h = 8, 10, 12, 15$ for simplicity. Details of our modeling and simulations are described in the Simulation Methods section. The reduced Lennard Jones units can be mapped onto physical units, such as for polystyrene, by taking $\sigma \approx 1$ to 2 nm, 1 time unit ≈ 9 to 18 ps, and $\varepsilon/k_B \approx 490$ K.⁴⁰

In previous studies on polymer thin films and nanocomposites, we focused on the relation between the degree of collective motion within the material and the structural relaxation time, as estimated from the intermediate scattering function. In particular, the T dependence of the activation free energy from relaxation time was determined from simulation, and this quantity was found to be consistent with the extent of collective motion in the form of string-

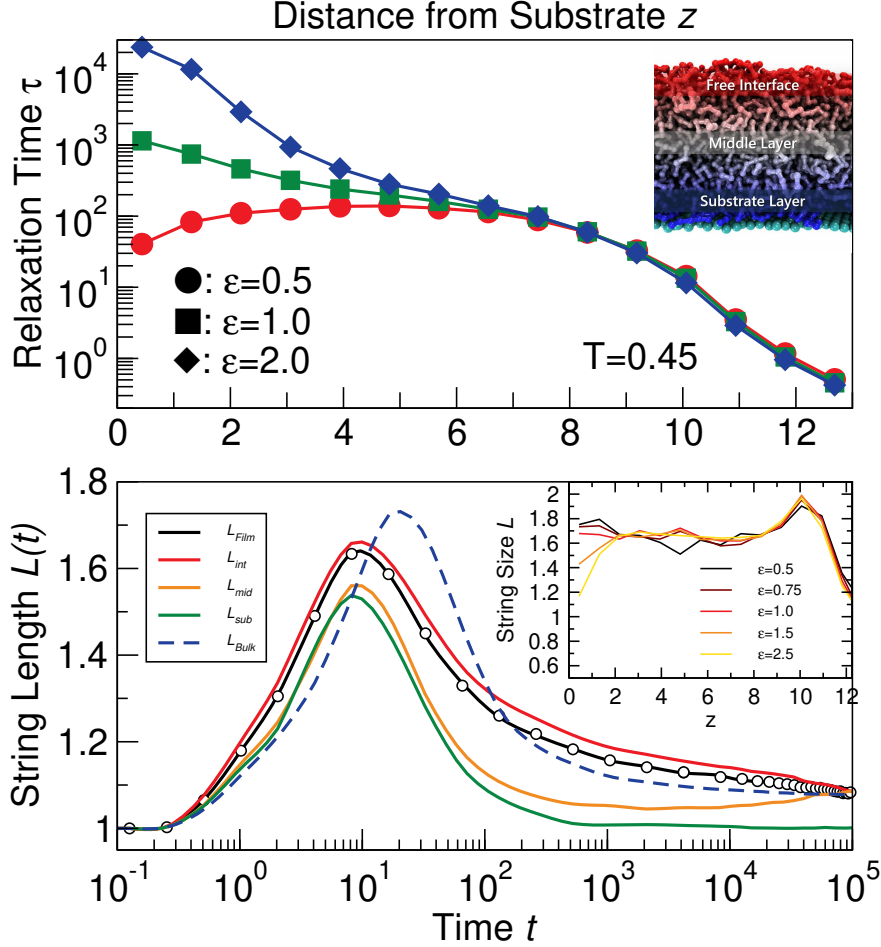


Figure 1: (a) The relaxation profile of polymer film with some representative polymer-substrate interaction strength ϵ values at $T = 0.45$. The thin polymer film in the picture has a thickness of roughly 12 nm with a strong substrate-polymer interaction strength $\epsilon = 2.0$. The picture also shows the schematic definition of free interface, middle, substrate layer, and substrate (turquoise). (b) The dynamical string length $L(t)$ for free interface, middle and substrate layers of the film, and film as a whole. The characteristic peak denotes time scale or “string lifetime”³⁷ and the peak string size, defining the string length L are similar for different parts of the film, despite the significant relaxation gradient within the film. The dashed line shows L for the bulk polymer under pressure $P = 0$. The inset shows the string size as a function of its center of mass position. It shows that the variation of string size is relatively small, and the string size is nearly the same when averaged over the interfacial regions.

like collective segmental exchange events,^{29,34} much as Adam-Gibbs has argued for intuitively in their theory of glass-formation.¹² We have found that this “string model” of glass-formation *quantitatively* describes relaxation over the computationally accessible temperature range for a broad range of systems (bulk polymers, thin supported films, and nanocomposites), as well

as variable material conditions [fixed pressure,^{41,42} constant volume,⁴³ and variable cohesive interaction⁴⁴]. The present work extends this approach to consider relaxation in *local* regions within a model glass-forming liquid.

We first examine the string-like collective motion $L(t)$ in thin polymer films as a function of both substrate interaction strength ε and thickness h , following procedures developed in earlier works.^{27,28} It has been shown that the string-like cooperative motion is a candidate to quantify cooperatively rearranging regions (CRRs), which follows the growth of the relaxation activation energy³⁷ and the average length of the strings L , defined by its peak value (See Fig. 1b) has been found to scale inversely to the configurational entropy to a good approximation,³⁷ consistent with basic assumptions made in the Adam-Gibbs model of glass formation when L is equated to the hypothetical CRR of this model. We consider the string length $L(t)$ for the film as a whole as well as in the free interfacial region, middle region, and substrate region, as shown in Fig. 1. From the approach described in Ref. 39, the thickness of the substrate layer h_{sub} nearly saturates for film thickness $h \gtrsim 8$. For simplicity, we choose substrate layer thickness $h_{\text{sub}} = 4.17$, or ≈ 4 nm in physical units for the range of film thickness in this study. In the case where there is no bound layer³⁸ near the substrate ($\varepsilon < 1.0$), we use the same value for h_{sub} , so that we can have a comparable scale to define the substrate layer relaxation and string length. The thickness of the “free” or polymer-air interfacial layer is defined by the top part of the film having a thickness of 3.5σ , corresponding to 3.5 to 7 nm. This layer has nearly the same relaxation time for films with different thickness h and polymer-substrate interaction strength ε . The middle layer is defined by the remaining part of the film (i.e. the film excluding the free interfacial and substrate layers). To examine the average string length L in different regions of the film, we first identify the strings from the whole film, and sort these strings spatially based on the position of the center of mass of each string. As illustrated in Fig. 1 the cooperative motion scale $L(t)$ and the timescale (t_L) at which string length peaks in each region, are nearly the same for the free interface, middle and substrate layers, in spite of differences in the ratio of

local relaxation time between substrate layer and free interfacial layer being as large as 10^5 . This observation is consistent with the notion that the thermodynamic CRR size is not a locally defined quantity. We note that in previous work based on the present polymer model in the bulk it was shown that L scales inversely proportional to S_c to a good approximation over the computationally accessible T range.³⁷

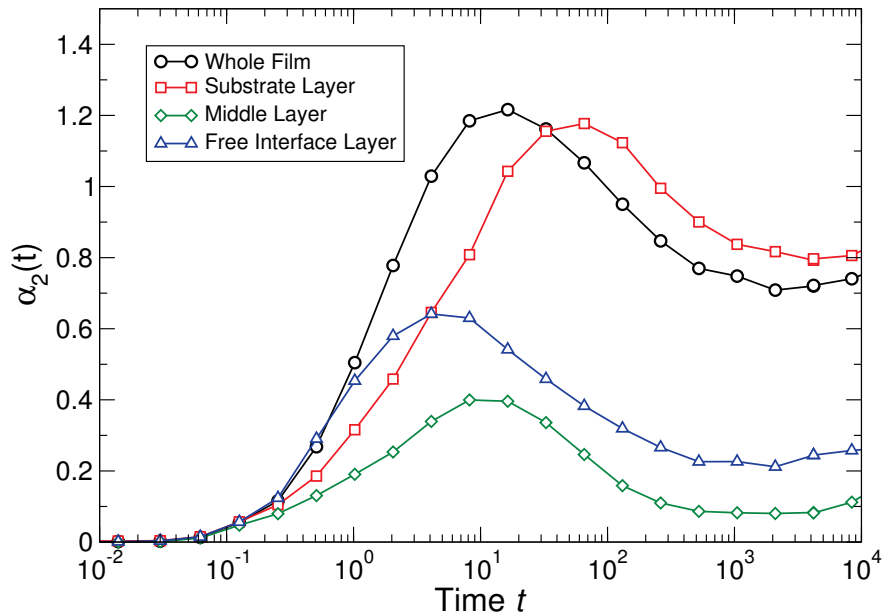


Figure 2: The non-Gaussian Parameter $\alpha_2(t)$ for free interface, middle and substrate layers of the film, and film as a whole at $T = 0.5$. The thin polymer film has thickness roughly equals to 12σ with a strong substrate-polymer interaction strength $\varepsilon = 2.0$. We use the same film and layer definition as that in Fig. 1.

It is important to clarify that the near uniformity of the scale of collective motion in our supported polymer films *does not imply* that “dynamical heterogeneity” within the film is uniform. We support this statement by considering a common metric of dynamical heterogeneity, the non-Gaussian parameter,

$$\alpha_2(t) = \frac{3 \langle \Delta \mathbf{r}^4(t) \rangle}{5 \langle \Delta \mathbf{r}^2(t) \rangle^2} - 1, \quad (1)$$

where $\langle \Delta \mathbf{r}^2(t) \rangle$ is the mean-square displacement of the monomers. This quantity peaks at a characteristic time t^* , related to diffusion in small molecular liquids,³⁷ and defines a

segmental mobility time scale for polymers.⁴¹ In general, t^* exhibits a power-law scaling in relation to the segmental relaxation time τ_α , i.e., $t^* \propto \tau_\alpha^\xi$, where $\xi < 1$, a phenomenon termed “decoupling”.^{34,45} As expected from the pronounced gradient of mobility, t^* and the height of the non-Gaussian parameter both vary strongly with their location in the film in Fig. 2. Note that $\alpha_2(t)$ does not vanish at large t for the film as a whole, or in the interfacial regions, owing to the gradient in mobility that persists over all time scales.²⁶

From an Adam-Gibbs perspective, collective molecular motion is important for understanding the structural relaxation in glass-forming systems. Naively, the apparent invariance of string size to location in the film would lead us to expect that the AG picture cannot be extended to understand the extreme variations in local relaxation. However, as we now discuss, the physical situation is more subtle. To apply the AG approach *locally*, we examine the dynamics of each film region using string model of relaxation in glass-forming materials,^{29,46} a modern extension of the Adam-Gibbs model founded on simulation evidence,

$$\tau(T) = \tau_0(\varepsilon, h) \exp \left[\frac{L(T)}{L_A} \frac{\Delta\mu(T)}{k_B T} \right], \quad (2)$$

where $\tau_0 = \tau_\beta(\varepsilon, h) \exp \left[\frac{-\Delta\mu(T_A)}{k_B T_A} \right]$ with $\tau_\beta \equiv \tau(T_A)$ and $\Delta\mu(T, \varepsilon, h) = \Delta H(\varepsilon, h) - T\Delta S(\varepsilon, h)$; T_A is the onset temperature of glass formation,^{29,37} and ΔH and ΔS are the high temperature enthalpic and entropic contributions of the free activation energy, respectively; τ_β is the fast β relaxation time, which equals the α -relaxation time τ_α at T_A .⁴⁷ In the bulk material, ΔH is directly related to the activation energy E_a determined from fitting relaxation time over high temperature region where relaxation is Arrhenius.⁴³ We utilize a fixed onset temperature $T_A = 0.65$ for thin films, as estimated in Ref. 46, since its value is relatively insensitive to polymer film thickness and polymer-substrate interaction strength. $L_A \equiv L(T_A)$ is the string length at the onset temperature T_A , the residual collective motion in the high temperature liquid.³⁴ Note that both L_A and τ_A depend on film thickness h , polymer-substrate interaction strength ε , as well as in the different regions of the film with, but the range of value is not

large, $L_A = 1.40 \pm 0.02$ and $\tau_A = 2.3 \pm 1.0$.²⁹ We emphasize that τ_0 is not a free fitting parameter, but τ_0 rather is determined³⁴ by ΔH and ΔS . It is also notable that τ_0 varies significantly with film thickness h , along with the supporting boundary interaction strength and stiffness.³⁴

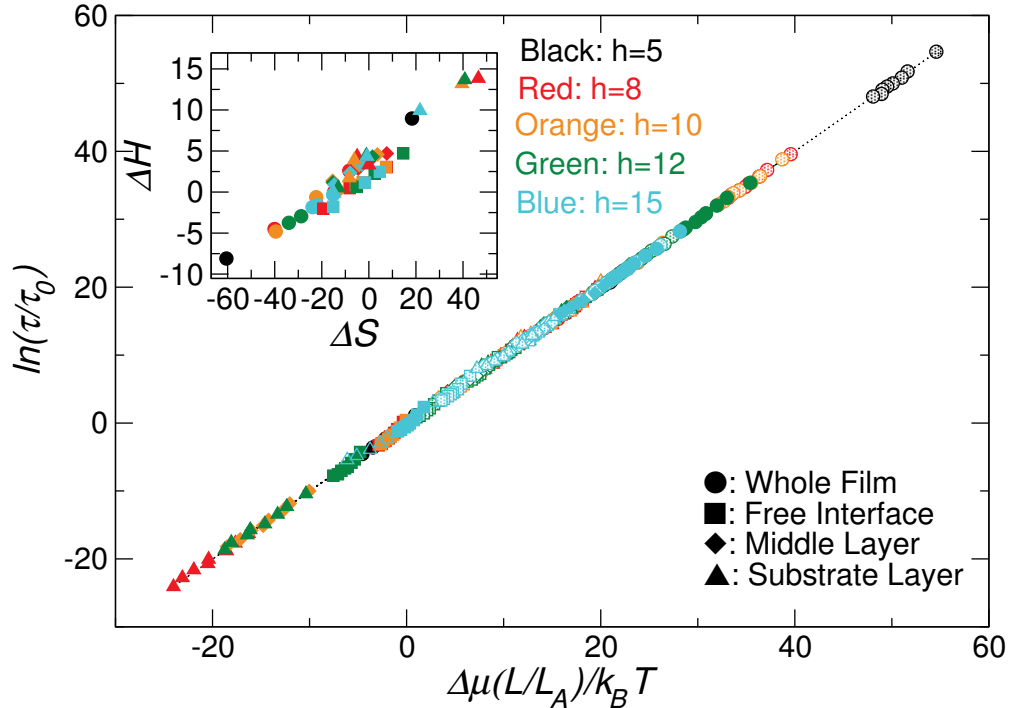


Figure 3: Test of string model for cooperative relaxation. Reduced relaxation time as a function of the reduced activation free energy for different film thicknesses, and regions of the film (free interfacial, middle and substrate layer). Hollow, dotted, and solid symbols stand for $\varepsilon = 0.5, 1.0,$ and $2.0,$ respectively. The inset shows the entropy-enthalpy compensation plot, obtained from fit to Eq. 2.

Although the approximate invariance of string size to location within the film does not explain the large variations in relaxation time within films, we may use Eq. 2 to understand the dynamics of thin polymer film for both film as a whole and local regions within it, and the relation of film relaxation to that of the bulk material. Figure 3 shows that there is a linear relationship between the reduced relaxation time $\ln(\tau/\tau_0)$ and the reduced activation energy $\frac{L(T)}{L_A} \frac{\Delta\mu}{k_B T}$ for various polymer-substrate interaction strength ε , film thickness h , and different local regions. A remarkable universal collapse of τ in term of string length was found in Refs. 29,32,34 for both thin polymer film and polymer nanocomposites. Note

that in the case of the extremely thin film with thickness $h = 5$, the free interfacial and substrate layer are not well-defined, so Fig. 3 does not include these interfacial regions. We thus find the string model of glass formation⁴⁶ can also quantitatively describe *local* film dynamics. The values of ΔH and ΔS (fitting parameters) that result from the application of Eq. 2 are shown in the inset of Fig. 3, which, when plotted parametrically, show that an entropy-enthalpy compensation relation ($\Delta S = \Delta S_0 + T_{\text{comp}}\Delta H$, where $T_{\text{comp}} \approx 0.21$) holds for different film regions as well. The value of T_{comp} obtained here is consistent with a previous estimate obtained from thin film and polymer nanocomposites simulations based on the same polymer model.²⁹

Large gradients and an entropy-enthalpy compensation relation have also been observed in the interfacial dynamics of crystalline Ni⁴⁸ and Cu⁴⁹ so that this phenomenon apparently arises in both crystalline and non-crystalline materials. Note that ΔH and ΔS estimates in the inset of Fig. 3 near the solid substrate can be negative. This counter-intuitive phenomenon has been observed in the kinetics of highly confined fluids when the interaction between the molecule and the boundary are strongly attractive.⁵⁰ Entropy-enthalpy compensation and negative values of ΔH and ΔS are also commonly observed in the thermodynamics of molecules binding,⁵¹ a counter-intuitive phenomenon associated with competitive molecular interactions. Previous work investigating the mobility gradient near the free interface of a crystalline material (Cu),⁴⁹ has quantified the mobility gradient in terms of a gradient in the activation free energy $\Delta\mu$, and we likewise consider the segmental relaxation time τ_α and activation free energy as a function of distance from the film free surface. In particular, if we take $z = 0$ to denote the position of the polymer interface and L to be the average value of the film as whole, then the string model prediction for the segmental relaxation time can be formally written,

$$\frac{\tau_\alpha(z)}{\tau_0(z)} = \left(\frac{\tau_\alpha^{\text{Film}}}{\tau_0^{\text{Film}}} \right)^{\frac{\Delta\mu(z)}{\Delta\mu^{\text{Film}}}}, \quad (3)$$

where $\tau_\alpha^{\text{Film}} = \tau_0^{\text{Film}} \exp \left[\frac{L(T)}{L_A} \frac{\Delta\mu^{\text{Film}}}{k_B T} \right]$ is the relaxation time for the film as a whole. The large gradient in the relaxation time τ_α within the polymer film within this model can thus be traced to a gradient in $\Delta\mu$ rather than a variation of the extent of collective motion as a function of distance within the film. Moreover, by averaging over interior and interfacial regions of the film, we obtain an extension of Eq. 3 that relates the ratio of interior and polymer-air interfacial relaxation times to the difference in the mean activation free energy in these regions, namely we have the relaxation time ratio,

$$\frac{\tau_{\text{mid}}}{\tau_{\text{int}}} = \frac{\tau_0^{\text{mid}}}{\tau_0^{\text{int}}} \exp \left[\frac{L(T)}{L_A} \frac{(\Delta\mu_{\text{mid}} - \Delta\mu_{\text{int}})}{k_B T} \right], \quad (4)$$

where $L(T)$ is again the characteristic string length of the film as a *whole*. This relation is potentially of significant practical value since the ratio $\tau_{\text{mid}}/\tau_{\text{int}}$ is experimentally accessible, and recent measurements have indicated that this mobility ratio can be as large as 10^7 near T_g .^{9,10} Note that Eq. 4 can be well-approximated as a Vogel-Fulcher-Tammann (VFT) function²⁴ over the computationally accessible temperature range, and we previously found this ratio to extrapolate to a value on the order of $\mathcal{O}(10^{11})$ as T approaches T_g .²⁶

While the extent of collective motion clearly changes with film thickness, we may still approximately relate relaxation within the film to relaxation of the bulk material. Provided the *ratio* L/L_A remains nearly the same in thin film and bulk material with $L_{\text{Bulk}}/L_A^{\text{Bulk}} \approx L_{\text{Film}}/L_A^{\text{Film}}$ (see Fig. 4), we then have the approximate relation:

$$\frac{\tau_\alpha(z)}{\tau_0(z)} \approx \left(\frac{\tau_\alpha^{\text{Bulk}}}{\tau_0^{\text{Bulk}}} \right)^{\frac{\Delta\mu(z)}{\Delta\mu^{\text{Bulk}}}}. \quad (5)$$

Figure 4 shows that the relative change in collective motion L/L_A is indeed similar in magnitude in the bulk and thin film for the temperature range and polymer-substrate interaction strength range. We emphasize that Eq. 5 is only suggested to be a reasonable *approximation* over the computationally accessible temperature range. Nonetheless, Eqs. 4 and 5 allow for an alternate understanding of previously observed computational evidence for a phe-

nomenclological power law or “decoupling” relation linking the relaxation time of the film as a whole to the relaxation times within the interfacial regimes and between the film as a whole and the bulk material.^{52–54} The near constancy of L/L_A between the bulk and thin films, along with the normally reduced molecular cohesive interaction strength at the polymer-air boundary, also naturally explains the near-Arrhenius relaxation in the interfacial region, its relatively high mobility in comparison to the bulk. It will be interesting to see whether the “decoupling” relation between wave-vector dependence of the relaxation time $\tau(q)$ from the intermediate scattering function to τ_α can likewise be understood in a similar fashion since the scale of collective motion must also be independent of observational scale.

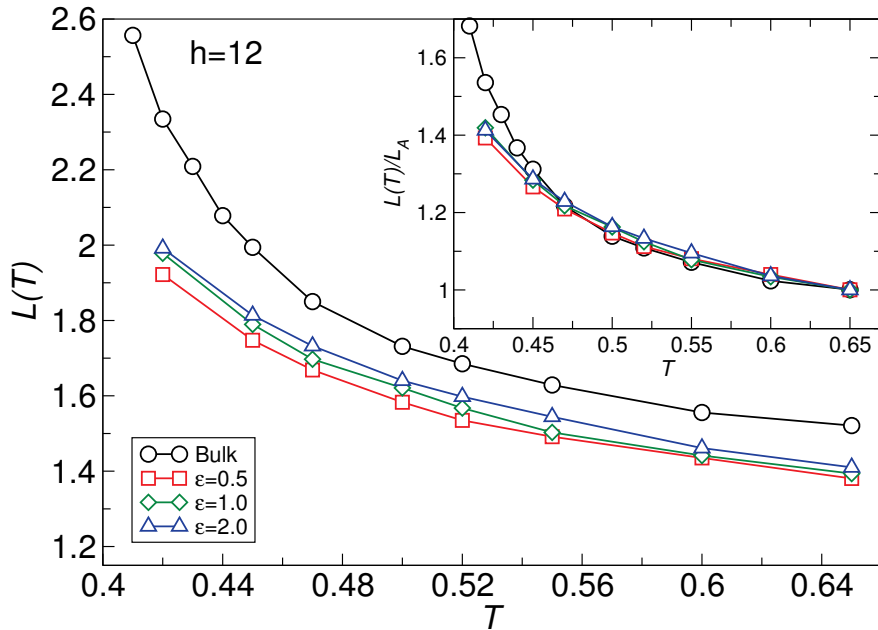


Figure 4: The characteristic string length $L(T)$ for polymer films as a whole with some representative polymer-substrate interaction strengths ($\varepsilon = 0.5, 1.0,$ and 2.0), and bulk polymer. The inset shows $L(T)$ normalized by their corresponding string length at the onset temperature L_A ($L_A \equiv L(T_A)$). Although confinement and polymer-surface interaction strength influence the scale of collective motion, the relative change in L is rather insensitive to their confinement and interfacial variables.

Conclusions

Our investigation of collective motion in relation to the internal dynamics of thin supported film provides further evidence of the importance of variations of the cohesive interaction in thin films for understanding both changes in relaxation in relation to the bulk and mobility gradients with these films. Changes in the cohesive interaction strength in the interfacial region are important because they alter the activation free energy $\Delta\mu$, which effects even the liquid regime far above the glass transition temperature.^{29,34} We find that many important aspects of the dynamics can be understood from interfacial changes of $\Delta\mu$, rather than changes in the scale of collective motion. Specifically, we find (i) a greatly enhanced mobility at the polymer-air interface in comparison to the bulk material, (ii) a near invariance of enhanced interfacial mobility with changes of film thickness, and (iii) the phenomenon of enthalpy-entropy compensation in the activation free energy parameters, ΔH and ΔS . The observation of a similarity in the degree of cooperative motion within the polymer-air interfacial region and the film interior is also theoretically interesting because it provides guidance regarding how to extend the Adam-Gibbs model to describe local mobilities within mesoscopic regions in glass-forming polymer films, and potentially nanocomposites. We plan to extend the analysis of the present paper to describe nanocomposites and to understand the physical origin of the width of the interfacial zones on the scale of collective motion found previously for both polymer films and nanocomposites.

An important practical implication of our work is the suggestion that local changes in the segmental dynamics can be understood primarily from changes dynamics of the Arrhenius activation free energy parameters characteristic of the fluid dynamics at elevated temperatures. Perhaps surprisingly, the extent of collective motion within the film does not vary substantially across the film profile, and accordingly does not contribute significantly to spatial variations in the local dynamics. Consequently, knowing the extent of collective motion for the material as a whole appears to be sufficient to understand change of material dynamics with confinement, if the changes to local activation parameters are additionally known. This

is good news, since, if one had to instead determine the degree of collective motion locally to understand local mobility variations, then the theory would be essentially intractable from a practical standpoint. The deduction of simple power-law relations between the segmental relaxation of the film as a whole only exists in the string model of glass-formation when the string length parameter of this model has no depth dependence. This is apparently the origin of both the decoupling relation in the string model of glass formation and the success of this model in fitting our simulation data for the relaxation time as function of depth over a wide range of temperatures. The fact that the spatial dependence of the cooperativity scale is not needed provides a readily implemented framework for studying mobility variations in glassy materials.

Of course, the general validity of this extended string model of glass-formation requires further confirmation in polymer nanocomposites and other types of non-uniform glass-forming materials to test the validity of this model. There is also a need to better understand the root physical causes of the gradients in the activation energy parameters given their large influence on the mobility gradients in thin films. In bulk materials, the high temperature activation enthalpy correlates very strongly with the cohesive energy density of the fluid, suggesting that these gradients in activation energy may derive physically from gradients in the potential energy density near the interfaces, which we are currently investigating. Further efforts are also required to understand the ubiquitous enthalpy-entropy compensation relation linking the activation enthalpy to activation entropy in the dynamics of many condensed materials. We suggest that more theoretical and experimental efforts should be devoted to understanding these fundamental energetic parameters.

Modeling and Simulation Details

Our results are based on molecular dynamics simulations of thin supported polymer films. We simulate supported thin polymer films with variable film thickness h and strength of

attractive interaction ε between the substrate and polymer employing molecular dynamics simulations. The polymer film model is the same as that used in Refs. 34,38. The polymer films have 320, 400, 480, or 600 polymer chains; these films have thicknesses $h \approx 5\sigma, 8\sigma, 10\sigma, 12\sigma$ and 15σ , respectively, which decrease approaching T_g . These films are referred to as $h = 8, 10, 12,$ and 15 . Above the film is free (empty) space, so the film is effectively at pressure, $P = 0$. As a reference for the thermodynamic and dynamic properties, we also simulated a bulk polymer with periodic boundary conditions in all directions at pressure $P = 0$.

Polymers are modeled as unentangled chains of 10 beads linked by harmonic springs. We use the harmonic spring potential $U_{\text{bond}} = \frac{k_{\text{chain}}}{2}(r - r_0)^2$ to connect nearest-neighbor monomers within a polymer chain. The equilibrium bond length is $r_0 = 0.9$ and the spring constant is $k_{\text{chain}} = 1111$.³⁴ To inhibit crystallization of the film, we choose r_0 smaller than that chosen in Ref. 55. We use the same substrate model as that in Ref. 38 for all the films studied. The substrate consists of 528 particles arranged in a triangular lattice (the (111) face of an FCC lattice). We tether substrate particles via a harmonic potential $V_{\text{sub}}(r) = (k/2)(r - r_0)^2$, where r_0 is the ideal lattice position and $k = 50$ is the spring constant.^{56,57} We use Lennard-Jones (LJ) interactions between non-bonded monomers and substrate particles. The interactions are truncated at pair separations $2.5\sigma_{ij}$, where σ_{ij} is equivalent to the particle diameter in the LJ potential, and the subscript ij indicates the possible combinations of interactions (ss substrate-substrate, ps polymer-substrate, pp polymer-polymer). All units are given relative to the strength ε and size σ of non-bonded polymer-polymer interactions. Consequently, T is in unit of ε/k_B , where k_B is Boltzmann's constant, pressure is in the unit of ε/σ^3 , and time in units of $\sqrt{m\sigma^2/\varepsilon}$. The LJ parameters are $\sigma_{pp} = 1.0$, $\varepsilon \equiv \varepsilon_{pp} = 1.0$, $\sigma \equiv \sigma_{ps} = 1.0$, $\sigma_{ss} = 0.8$, $\varepsilon_{ss} = 1.0$, and we use interaction strengths between monomers and substrate particles $\varepsilon_{ps} = 0.1, 0.25, 0.5, 0.75, 1.0, 1.25, 1.5, 2.0, 2.5,$ and 3.0 . Since we only vary ε_{ps} , we simply refer to this quantity as ε .

Periodic boundary conditions are used in the directions parallel to the substrate with a

box length 19.76σ (determined by the lattice spacing of the triangular lattice substrate). We conducted all simulations using the LAMMPS⁵⁸ simulation package with a time step $dt = 0.002$. For cooling and heating simulations of the bulk polymers, we use an NPT ensemble at $P = 0$. We performed at least 3 independent heating and cooling runs for both the pure polymer and polymer films at the same rate 10^{-5} . To generate trajectories from which we study the dynamics at fixed T , we carry out NPT simulations starting from configurations taken from the heating runs at $T > T_g$ with pressure $P = 0$. For the supported polymer films, we use an NVT ensemble where the box dimension in the z -direction is large compared to the film thickness. The temperatures are varied from 0.45 to 0.65, above (the heating rate dependent) $T_g(h = 15) \approx 0.40$ of the thickest polymer film.³⁸ We equilibrate each trajectory for at least 100 times the average polymer relaxation time of the entire film τ_{overall} .

Acknowledgement

Computer time was provided by Wesleyan University. This work was supported in part by NIST Award No. 70NANB15H282.

References

- (1) Sharp, J. S.; Forrest, J. A. *Physical Review Letters* **2003**, *91*, 235701.
- (2) Ediger, M. D.; Forrest, J. A. *Macromolecules* **2014**, *47*, 471–478.
- (3) DeMaggio, G.; Frieze, W.; Gidley, D.; Zhu, M.; Hristov, H.; Yee, A. *Physical Review Letters* **1997**, *78*, 1524–1527.
- (4) Priestley, R. D.; Ellison, C. J.; Broadbelt, L. J.; Torkelson, J. M.; M., T. J. *Science* **2005**, *309*, 456–459.

- (5) Hesami, M.; Steffen, W.; Butt, H.-J.; Floudas, G.; Koynov, K. *ACS Macro Letters* **2018**, *7*, 425–430.
- (6) Napolitano, S.; Glynos, E.; Tito, N. B. *Reports on Progress in Physics* **2017**, *80*, 036602.
- (7) Zhu, L.; Brian, C.; Swallen, S.; Straus, P.; Ediger, M.; Yu, L. *Physical Review Letters* **2011**, *106*, 256103.
- (8) Paeng, K.; Richert, R.; Ediger, M. *Soft Matter* **2012**, *8*, 819–826.
- (9) Brian, C. W.; Yu, L. *The Journal of Physical Chemistry A* **2013**, *117*, 13303–13309.
- (10) Zhang, Y.; Fakhraai, Z. *Proceedings of the National Academy of Sciences* **2017**, *114*, 4915–4919.
- (11) Bell, R. C.; Wang, H.; Iedema, M. J.; Cowin, J. P. *Journal of the American Chemical Society* **2003**, *125*, 5176–5185.
- (12) Adam, G.; Gibbs, J. H. *The Journal of Chemical Physics* **1965**, *43*, 139–146.
- (13) Shavit, A.; Douglas, J. F.; Riggleman, R. A. *The Journal of Chemical Physics* **2013**, *138*, 12A528.
- (14) Riggleman, R. A.; Yoshimoto, K.; Douglas, J. F.; de Pablo, J. J. *Physical Review Letters* **2006**, *97*, 045502.
- (15) Shavit, A.; Riggleman, R. A. *The Journal of Physical Chemistry B* **2014**, *118*, 9096–9103.
- (16) Gibbs, J. H.; DiMarzio, E. A. *The Journal of Chemical Physics* **1958**, *28*, 373–383.
- (17) Xu, W.-S.; Douglas, J. F.; Freed, K. F. *Advances in Chemical Physics* **2016**, *161*, 443–497.
- (18) Jackson, C. L.; McKenna, G. B. *Journal of Non-Crystalline Solids* **1991**, *131*, 221–224.

- (19) Salez, T.; Salez, J.; Dalnoki-Veress, K.; Raphaël, E.; Forrest, J. A. *Proceedings of the National Academy of Sciences* **2015**, *112*, 8227–8231.
- (20) Capaccioli, S.; Ngai, K.; Paluch, M.; Prevosto, D. *Physical Review E* **2012**, *86*, 051503.
- (21) Ngai, K.; Rizos, A.; Plazek, D. *Journal of Non-Crystalline Solids* **1998**, *235*, 435–443.
- (22) Ellison, C. J.; Ruszkowski, R. L.; Fredin, N. J.; Torkelson, J. M. *Physical Review Letters* **2004**, *92*, 095702.
- (23) Arutkin, M.; Raphaël, E.; Forrest, J. A.; Salez, T. *Soft matter* **2016**, *13*, 141–146.
- (24) Williams, M. L.; Landel, R. F.; Ferry, J. D. *Journal of the American Chemical Society* **1955**, *77*, 3701–3707.
- (25) Yang, Z.; Fujii, Y.; Lee, F. K.; Lam, C.-H.; Tsui, O. K. *Science* **2010**, *328*, 1676–1679.
- (26) Zhang, W.; Douglas, J. F.; Starr, F. W. *The Journal of Chemical Physics* **2017**, *146*, 203310.
- (27) Donati, C.; Douglas, J. F.; Kob, W.; Plimpton, S. J.; Poole, P. H.; Glotzer, S. C. *Physical Review Letters* **1998**, *80*, 2338.
- (28) Aichele, M.; Gebremichael, Y.; Starr, F. W.; Baschnagel, J.; Glotzer, S. *The Journal of Chemical Physics* **2003**, *119*, 5290–5304.
- (29) Pazmiño Betancourt, B. A.; Hanakata, P. Z.; Starr, F. W.; Douglas, J. F. *Proceedings of the National Academy of Sciences* **2015**, *112*, 2966–2971.
- (30) Betancourt, B. A. P.; Douglas, J. F.; Starr, F. W. *Soft Matter* **2013**, *9*, 241–254.
- (31) Zhang, H.; Zhong, C.; Douglas, J. F.; Wang, X.; Cao, Q.; Zhang, D.; Jiang, J.-Z. *The Journal of chemical physics* **2015**, *142*, 164506.
- (32) Hanakata, P. Z.; Douglas, J. F.; Starr, F. W. *Nature Communications* **2014**, *5*, 4163.

- (33) Zhang, H.; Khalkhali, M.; Liu, Q.; Douglas, J. F. *The Journal of chemical physics* **2013**, *138*, 12A538.
- (34) Hanakata, P. Z.; Pazmiño Betancourt, B. A.; Douglas, J. F.; Starr, F. W. *The Journal of Chemical Physics* **2015**, *142*, 234907.
- (35) Starr, F. W.; Sastry, S.; Douglas, J. F.; Glotzer, S. C. *Physical review letters* **2002**, *89*, 125501.
- (36) Hanakata, P. Z.; Douglas, J. F.; Starr, F. W. *The Journal of chemical physics* **2012**, *137*, 244901.
- (37) Starr, F. W.; Douglas, J. F.; Sastry, S. *The Journal of Chemical Physics* **2013**, *138*, 12A541.
- (38) Zhang, W.; Douglas, J. F.; Starr, F. W. *The Journal of Chemical Physics* **2017**, *147*, 044901.
- (39) Zhang, W.; Douglas, J. F.; Starr, F. W. *Proceedings of the National Academy of Sciences* **2018**, *115*, 5641–5646.
- (40) Kröger, M. *Physics reports* **2004**, *390*, 453–551.
- (41) Xu, W.-S.; Douglas, J. F.; Freed, K. F. *Macromolecules* **2017**, *50*, 2585–2598.
- (42) Xu, W.-S.; Douglas, J. F.; Freed, K. F. *ACS Macro Letters* **2016**, *5*, 1375–1380.
- (43) Xu, W.-S.; Douglas, J. F.; Freed, K. F. *Macromolecules* **2016**, *49*, 8355–8370.
- (44) Xu, W.-S.; Freed, K. F. *Macromolecules* **2014**, *47*, 6990–6997.
- (45) Henritzi, P.; Bormuth, A.; Klameth, F.; Vogel, M. *Journal of Chemical Physics* **2015**, *143*.

- (46) Pazmiño Betancourt, B. A.; Douglas, J. F.; Starr, F. W. *The Journal of Chemical Physics* **2014**, *140*, 204509.
- (47) Pazmiño Betancourt, B. A.; Starr, F. W.; Douglas, J. F. *The Journal of Chemical Physics* **2018**, *148*, 104508.
- (48) Zhang, H.; Yang, Y.; Douglas, J. F. *The Journal of Chemical Physics* **2015**, *142*, 084704.
- (49) Papageorgiou, D.; Evangelakis, G. *Surface Science* **2000**, *461*, L543–L549.
- (50) Artioli, N.; Lobo, R. F.; Iglesia, E. *The Journal of Physical Chemistry C* **2013**, *117*, 20666–20674.
- (51) Dudowicz, J.; Douglas, J. F.; Freed, K. F. *The Journal of Chemical Physics* **2018**, *149*, 044704.
- (52) Phan, A. D.; Schweizer, K. S. *Macromolecules* **2018**, *51*, 6063–6075.
- (53) Diaz-Vela, D.; Hung, J.-H.; Simmons, D. S. *ACS Macro Letters* **2018**, *7*, 1295–1301.
- (54) Chung, J. Y.; Douglas, J. F.; Stafford, C. M. *The Journal of Chemical Physics* **2017**, *147*, 154902.
- (55) Peter, S.; Meyer, H.; Baschnagel, J. *Journal of Polymer Science Part B: Polymer Physics* **2006**, *44*, 2951–2967.
- (56) Baschnagel, J.; Varnik, F. *Journal of Physics: Condensed Matter* **2005**, *17*, R851.
- (57) Varnik, F.; Binder, K. *Journal of Chemical Physics* **2002**, *117*, 6336–6349.
- (58) Plimpton, S. *Journal of Computational Physics* **1995**, *117*, 1–19.